

Article

Effect of Block Geometry and Divergence of Baffled Chute on Downstream Scour Pattern

Morteza Karimi Chahartaghi¹, Sohrab Nazari² and Mohsen Solimani Babarsad³

¹ Ph.D Student, Department of Civil Engineering- Water Resources Engineering and Management, Shoushtar Branch, Islamic Azad University, Shoushtar, Iran; morteza.karimich1@yahoo.com

² Assistant Professor, Department of Civil Engineering, Eghlid Branch, Islamic Azad University, Eghlid, Iran; Corresponding Author; nazari.soh@gmail.com

³ Assistant Professor, Department of Civil Engineering- Water Resources Engineering and Management, Shoushtar Branch, Islamic Azad University, Shoushtar, Iran; mohsen.solb@gmail.com

Abstract: The effect of divergence of chute sidewalls with three different baffle block geometries namely USBR, trihedral and semicircular blocks, as well as the depth and dimensions of the scour hole downstream of the chute were studied using a physical model. For this purpose, 9 models of baffled chutes were designed and constructed with divergence ratios of 1.45, 1.75, and 2.45 and without divergence (with a divergence ratio of 1). Comparing the results on the effect of block geometry at different divergence ratios revealed that the use of blocks proposed in this study instead of standard USBR blocks reduced the mean and maximum scour hole by 50%. For a given block geometry, the mean depth, maximum depth, and length of scour hole were reduced by 75%, 58%, and 50%, respectively.

Keywords: Physical model; chute structure; scour hole; divergence; downstream

1. Introduction

Erosion and scour downstream of hydraulic structures have always been a matter of concern for hydraulic engineers and researchers in this field. In addition to causing instability in structures and river side walls, erosion downstream of hydraulic structures may disrupt the function of structures through changes in the river topography. Spillways are among the most vulnerable structures in this regard as they are usually exposed to high-speed and high-energy currents with a high potential of erosion and destruction downstream of spillways. Numerous studies have been conducted on scour and its various aspects such as energy dissipation downstream of structures [1,6,14]. [3] reviewed studies by [1] on scour downstream of control structures. [4] experimentally examined scour downstream of a spillway with an apron installed at the end of spillway on the surface of sediments. According to their results, secondary flows downstream of the spillway formed several scour holes, which were gradually developed and jointed. Rock blocks can be used to enhance energy dissipation on the ramp as pointed out by [9,10]. [14]

studied the effect of adding baffles and end sills on energy dissipation of flow over stepped spillways with sharp or round edges and an ogee inlet. They found that a higher energy dissipation rate can be achieved in baffle-edge chutes as compared with sill-edge chutes as well as round- and sharp-stepped spillways. A chute structure with baffled blocks is considered a flow energy dissipator of impact type. A baffle block chute does not reduce velocity, but prevents flow acceleration so that a low-energy flow reaches downstream of the structure [12]. This structure was primarily suggested for a maximum discharge of $5.6 \text{ m}^3/\text{s}$ per unit width [12]. However, according to experiments conducted by other researchers employing dam spillway hydraulic models, this structure was later proposed for use at higher discharge rates [2]. The United States Bureau of Reclamation (USBR) has conducted extensive studies on baffle block chutes to achieve an optimal design. Note that the USBR guidelines recommend a slope of 2:1 for chutes [12]. Figure 1 displays the details of a chute structure with baffle blocks.

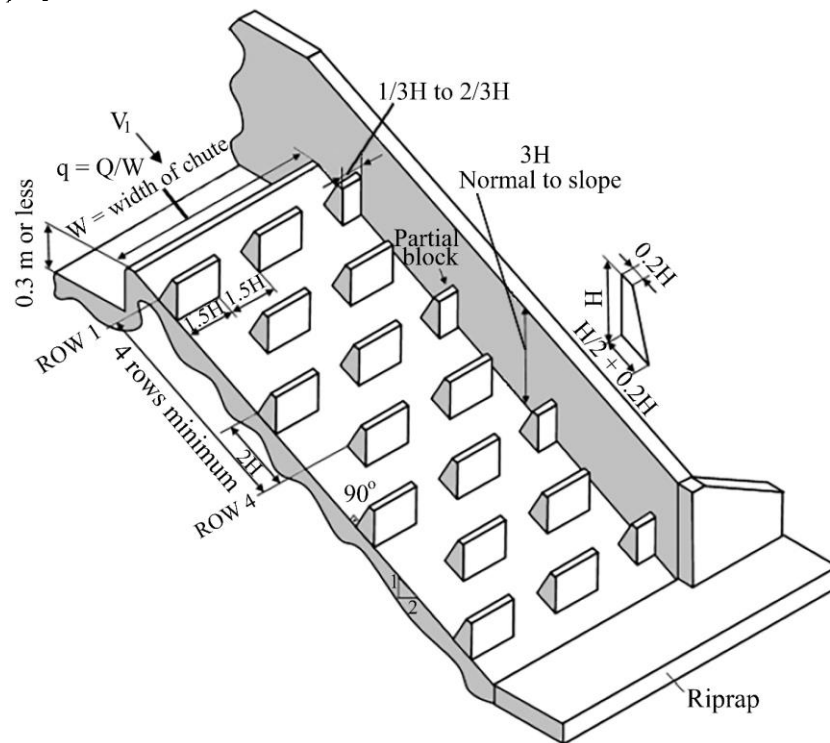


Figure 1. The components of a chute with trapezoidal baffle blocks [7].

[13] studied the effect of inlet channel angle of stepped spillways relative to the horizon on erosion downstream of spillways and found an optimal angle of 30° . [5] examined the effect of cylindrical blocks installed on the ramp downstream of spillway on the dimensions of scour hole downstream of the blocks. The effect of cylindrical block size and arrangement was explored at different discharges to obtain the optimal geometry and arrangement of cylinders. [7] investigated the effect of stepped, wedge, T-shaped, and trapezoidal blocks at different chute bed slopes from 1:4.24 to 1:0.73 on energy dissipation of the flow passing over this structure. According to their results, T-shaped blocks outperformed other geometries in terms of enhanced energy dissipation and oxygen level.

Due to spatial limitations in some circumstances, the structure is constructed divergent with a variable width. Further, efforts for enhancing efficiency of such structures have led to the use of blocks of various geometries. According to the literature, there is no study on the performance and scour downstream of divergent chutes with baffle blocks as along with the blocks proposed in the present study. This study aims at investigating the effect of divergence of chutes with semicircular and trihedral blocks and trapezoidal piers (USBR) on the scour rate and dimensions of scour hole. For this purpose, fixed and divergent laboratory models with different bed blocks and divergence ratios were tested at seven discharge rates after which the results were evaluated by dimensional analysis.

2. Materials and Methods

2.1. Dimensional analysis

The tested parameters are presented in Eq. (1):

$$\emptyset = f(Fr_0, d_s, L_s, V_s, H, y_c, b_2, b_1, h_b) \quad (1)$$

Where, d_s represents the mean and maximum scour depth, H shows head upstream of spillway in the reservoir, L_s denotes scour hole length, V_s is scour hole volume, (y_c) refers to critical depth of flow over the spillway, (Fr_0) is Froude number of the flow upstream of the spillway, (h_b) represents block height approximately equal to 0.8 (y_c), b_2 is spillway width downstream of the chute, and b_1 denotes spillway width upstream of the inlet. According to dimensional analysis by π -Buckingham theorem, Eq. (2) shows the relationship between the scour hole parameters downstream of the chute and baffle blocks:

$$\frac{d_s}{H}, \frac{L_s}{H}, \frac{V_s}{H^3} = f\left(\frac{y_c}{H}, Fr_0, \frac{b_2}{b_1}, \frac{h_b}{H}\right) \quad (2)$$

2.2. Apparatus and Methods

Experiments were conducted in a laboratory channel equipped with a water circulation system Figure 2 with a width of 1 m, length of 6 m, and height of 1.2 m. Water was injected into the system by a 5" centrifugal pump. A honeycomb baffle was installed at channel inlet for flow laminarization. After passing over the chute model, the flow was transferred to an underground tank to be recirculated by the centrifugal pump. The discharge rate was measured by an electromagnetic flowmeter with an accuracy of 0.01 L/s. To examine scour of sediments downstream of the chute, sand sediments with an average diameter (d_{50}) of 1.2 mm and a height of 0.15 m, length of 2 m, and width of 0.975 m were placed in this section.

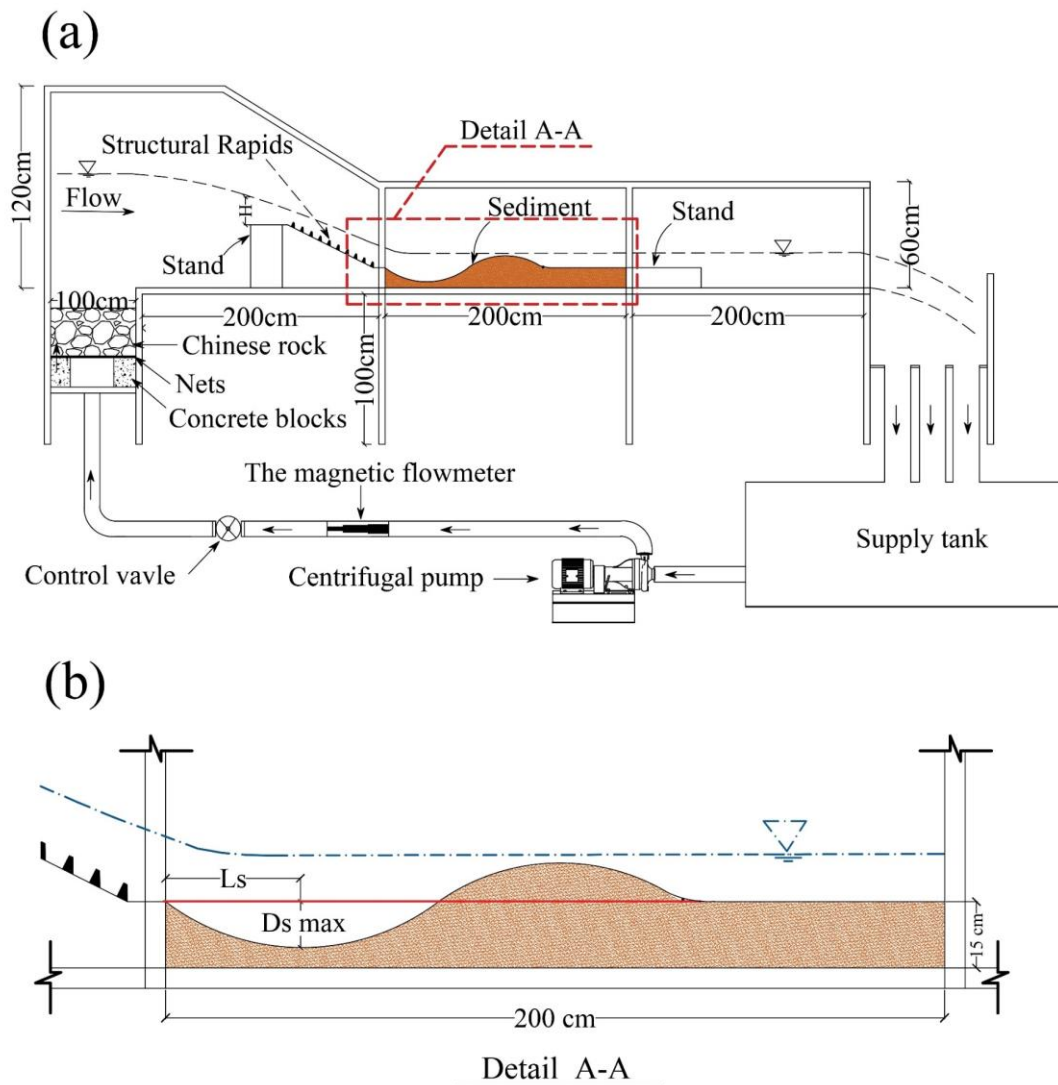


Figure 2. The detail of experimental flume and the place of installing the chute structure: (a) Longitudinal profile of the laboratory flume and equipment used with baffle block chute and (b) sediment bed downstream of the chute.

The wooden baffle piers were constructed and placed on the model according to the dimensions specified in USBR guidelines as presented in Figure 3. Ten labyrinth block rows were considered on the chutes. The approaching velocity over the chute should be sufficiently lower than the critical velocity. A short stilling basin with an end step of height 5 cm was considered to establish a laminar flow at chute model inlet. The head at upstream along and downstream of the divergent chute was measured by a point level gage with an accuracy of 0.1 mm. A block height of 4.3875 cm was considered in all models.

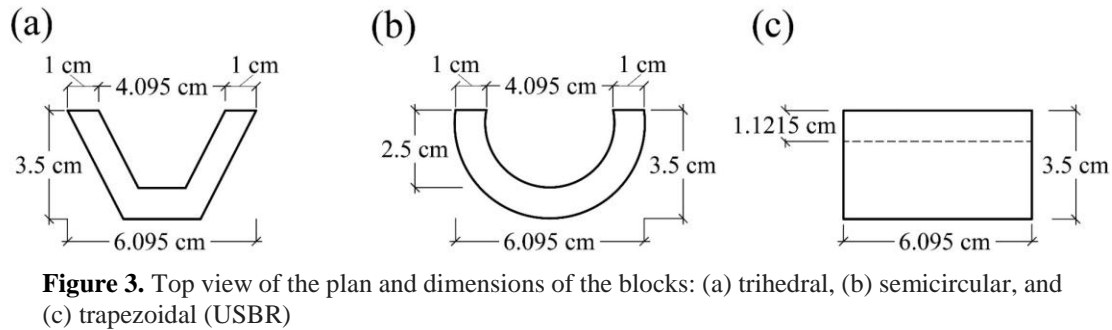


Figure 3. Top view of the plan and dimensions of the blocks: (a) trihedral, (b) semicircular, and (c) trapezoidal (USBR)

Three divergence ratios of 1.45, 1.75, and 2.45 and 1 (a fixed chute without divergence) were designed and tested according to Table 1 and Figure 4. A constant chute bed slope of 2:1 was used in all experiments. The number of blocks on the divergent models differed given their different surface areas. The detailed characteristics of the models are presented in Table 1.

Table 1. Dimensions and characteristics of the models constructed on the chute tested in the laboratory.

	Model and Block geometry	L (cm)	Z (cm)	b1 (cm)	b2=W (cm)	b2/b1	Number of blocks on the chute	Chute bed slope
1	Constant Width-USBR Block (CW-USB)	103.15	-	97.5	97.5	1	80	2:1
2	Constant Width-Semi Circle Block (CW-SCB)	103.15	-	97.5	97.5	1	80	2:1
3	Constant Width-Trihedral Block (CW-TRB)	103.15	-	97.5	97.5	1	80	2:1
4	Semi-Circle -Diverging Width 1 Block (DW1- SCB)	103.15	15.9	67.25	97.5	1.45	69	2:1
5	Diverging Width 1- Trihedral Block (DW1- TRB)	103.15	15.9	67.25	97.5	1.45	69	2:1
6	Semi-Circle -Diverging Width 2 Block (DW2- SCB)	103.15	19.2	55.08	97.5	1.75	65	2:1
7	Diverging Width 2- Trihedral Block (DW2- TRB)	103.15	19.2	55.08	97.5	1.75	65	2:1
8	Semi-Circle -Diverging Width 3 Block (DW3- SCB)	103.15	28.43	39.80	97.5	2.45	58	2:1
9	Diverging Width 3- Trihedral Block (DW3- TRB)	103.15	28.43	39.80	97.5	2.45	58	2:1

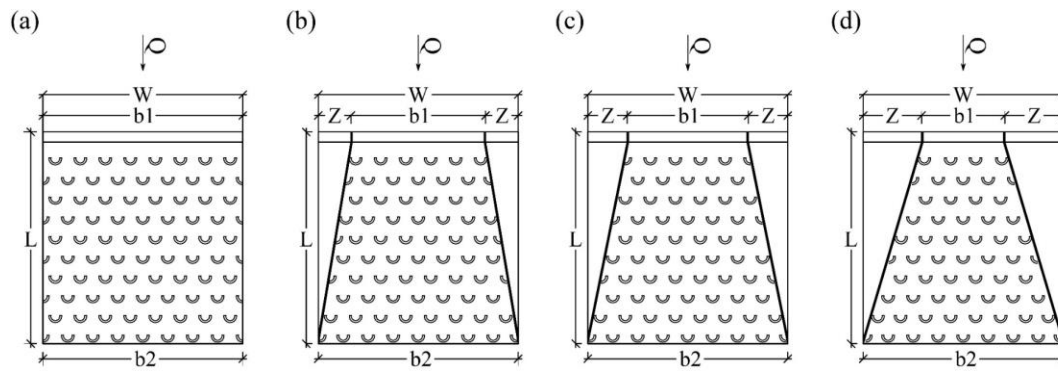


Figure 4. The plan and dimensions of the chute with different opening ratios and semicircular blocks: (a) $b_2/b_1=1$, (b) $b_2/b_1=1.45$, (c) $b_2/b_1=1.75$, (d) $b_2/b_1=2.45$.

Figure 5 demonstrates the laboratory models and arrangement of the chute components and sedimentary zone at downstream.

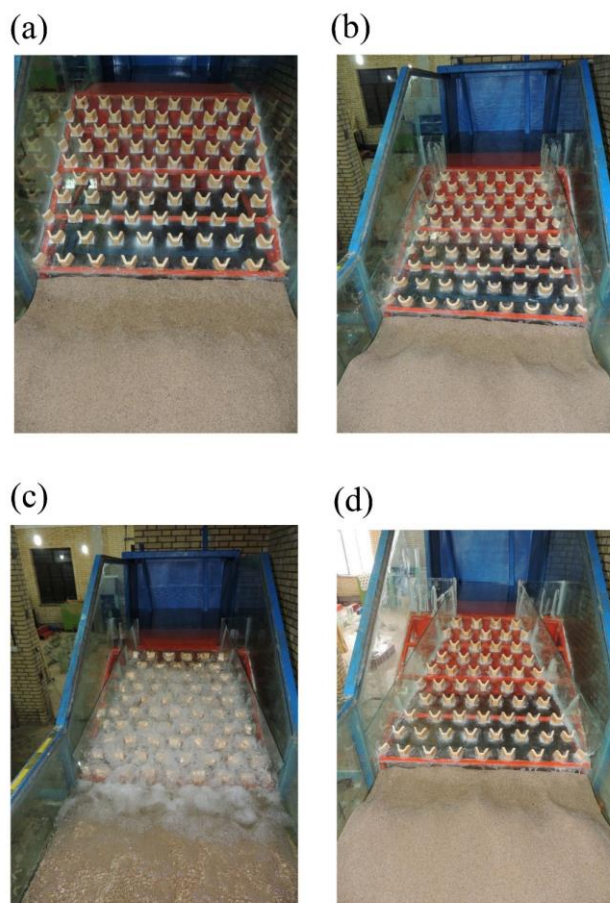


Figure 5. The baffled chute: (a) $b_1/b_2=1$ with a trihedral block, (b) $b_1/b_2=1.45$ with a semicircular block, (c) $b_1/b_2=1.75$ with a USBR block, (d) $b_1/b_2=2.45$ with a trihedral block.

To determine the optimal duration of experiments, a control experiment was first performed for 4 hr where the scour depth was recorded over time. Figure 6 shows the changes in the maximum scour depth with respect to time. As clearly seen, the changes disappear after 120 min, thus, all experiments were carried out within 120 min. After each experiment, a vehicle (chariot) moving along x and y axes with a laser meter was used to record the scour hole and point bar topographies, after which the collected data were analyzed.

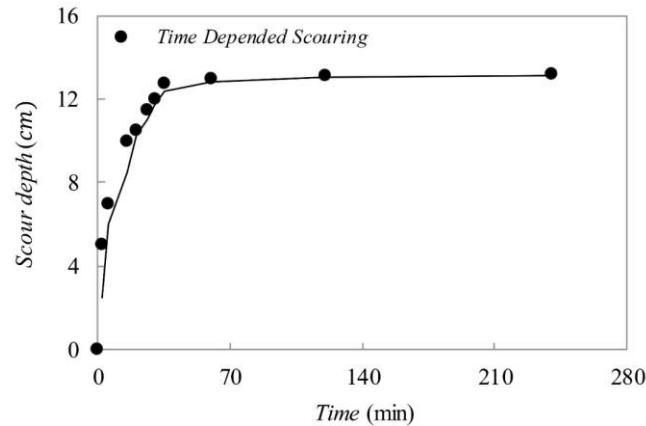


Figure 6. The changes in the scour depth with time.

To ensure the accuracy of data obtained from the laboratory model, the results obtained from the chute model without blocks were compared with those obtained from the relations in Table 2 presented by other studies with their data indicated in Figure 7. According to the results, (d_{smax}/H) rises with increasing (y_c/H) , suggesting that the maximum scour depth downstream of the chute grows with increasing the discharge rate. The results of this study are consistent especially with those obtained by [8].

Table 2. Relations for determining the scour depth downstream of hydraulic structures [5].

Source	Year	proposed equation
<i>Schoklitsh</i>	1932	$d_s + y_t = \frac{c_s q^{0.57} H^{0.2}}{d_{90}^{0.32}}$
<i>Novak</i>	1961	$d_s = 0.55(6H^{0.25} q^{0.5} (\frac{y_t}{d_{90}})^{1/3} - y_t$
<i>Kotulas</i>	1967	$d_s = 0.78 \frac{y_t^{0.35} q^{0.7}}{d_{90}^{0.4}}$
<i>Wu</i>	1973	$\frac{d_s}{H} = 2.11 \left(\frac{q}{(gH^3)^{1/2}} \right)^{0.51}$

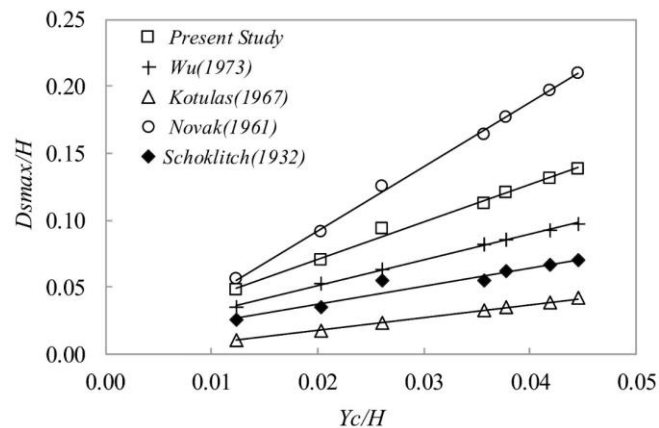


Figure 7. The relationship between dimensionless critical depth and maximum scour depth obtained in this study and from relations in the literature.

Experiments were conducted at seven discharge rates from 3 to 25 L/s on 9 different models with rigid blocks of different geometries with and without divergence. The results were presented as dimensionless figures. The scour hole depth and length as well as energy dissipation were also compared and discussed.

3. Results and Discussion

3.1. Bed topography

Using data on scour and sedimentation downstream of the laboratory models, the longitudinal profiles of bed scour were plotted at different discharges and divergence ratios, as shown in Figures 8 and 9. Figure 8 displays the longitudinal scour profiles at 6.5, 9.5, and 15.5 L/s for three types of blocks without divergence. In all cases, the standard blocks indicate the maximum scour depth along the flume centerline. Accordingly, one can conclude that the use of proposed blocks significantly decreases the maximum scour depth.

Figure 9 reveals the longitudinal scour profiles for semicircular blocks at different divergence ratios at 6.5, 9.5, and 15.5 L/s. As can be seen, the divergence causes an increase in the scour depth in the middle of channel as compared with the non-divergent model. However, the maximum scour depth was observed for DW1 divergence, where the scour rate decreased with elevation of the divergence ratio. Further, an ordered scour hole is formed with raising the divergence ratio. Despite formation of a set of holes in the non-divergent model, a single hole is formed as the divergence ratio grows. With elevation of the divergence ratio (b_2/b_1) up to 2.45, a deeper scour hole is formed at 6.5 L/s compared to 9.5 L/s.

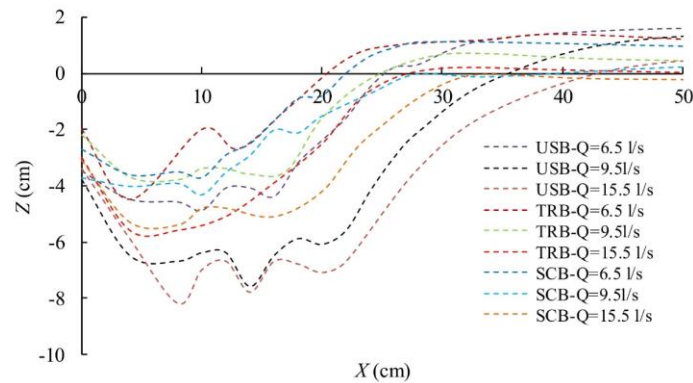


Figure 8. Comparison of the longitudinal scour profiles at three discharges and an opening ratio of 1 for three block geometries.

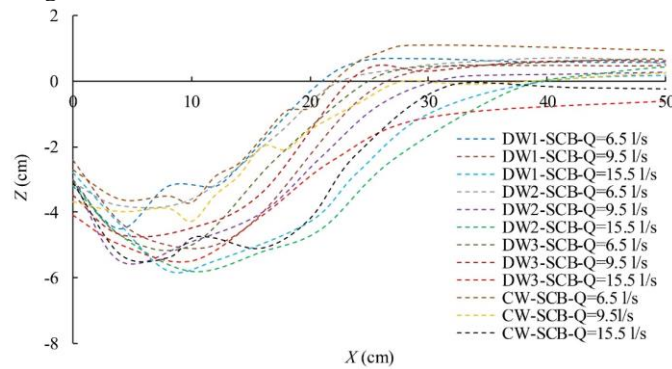


Figure 9. Comparison of the longitudinal scour profiles at three discharges and opening ratios for a semicircular block.

Figures 10 and 11 reveal the topography of the scour hole downstream of the chute at a discharge rate of 15 L/s. According to the results on the bed topography, an asymmetric scour hole has been formed along the channel width with a maximum depth on both sides of the channel centerline. The topography of the scour hole for the chute with semicircular blocks at different divergence ratios suggests that unlike the non-divergent model, the maximum scour hole occurs in the vicinity of the walls as the divergence ratio grows. Further, with an increase in the divergence ratio, the point bars begin to approach the walls presumably due to the formation of secondary flows colliding with the walls, causing scour, and transporting scour-induced sediments downstream of the side walls.

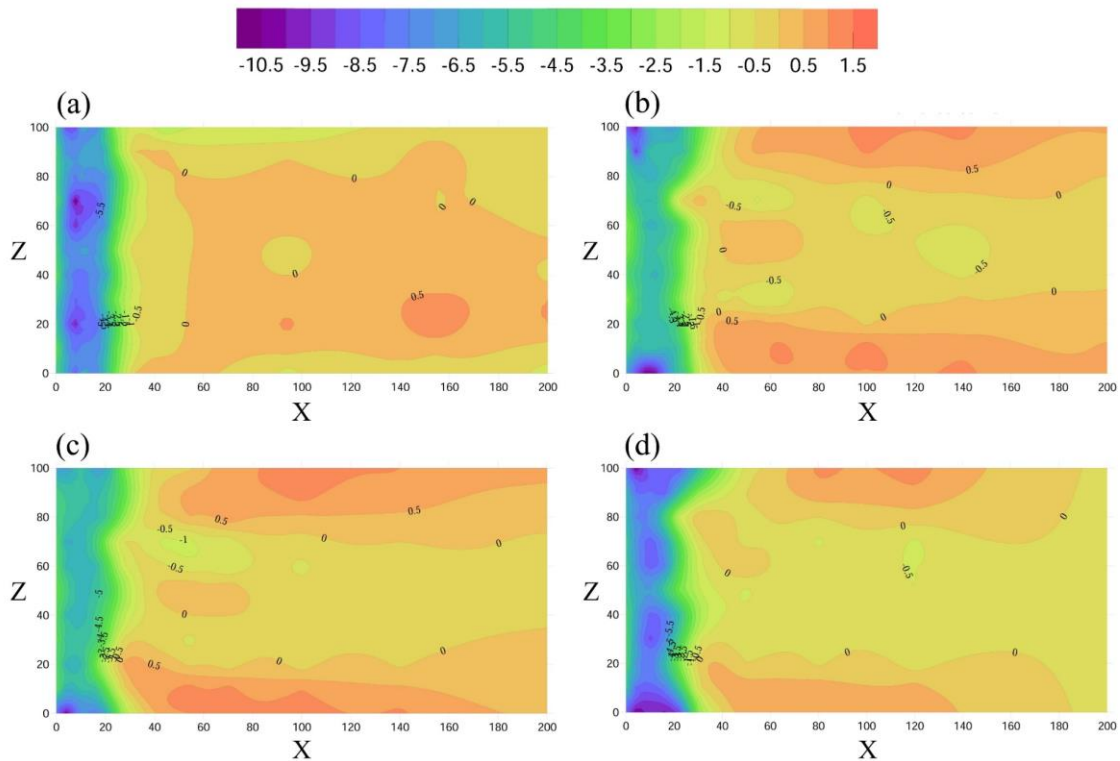


Figure 10. The bed topography for a chute with a semicircular block at a discharge of 15 L/s and different divergence ratios of (a) 1, (b) 1.45, (c) 1.75, and (d) 2.45.

Figure 11 shows the topography of the eroded beds for the non-divergent chutes with various block geometries. As can be seen, in the case where a standard block is used, the maximum scour hole length occurs in the middle of the channel and a large point bar is formed downstream of the scour hole in the middle of the channel. However, when semicircular and trihedral blocks are employed rather than the USBR standard block, the scour hole extends on both sides tangential to the side walls. The scour hole is further extended downstream of the chute towards the channel centerline. Despite a decrease in the depth and length of the scour hole at its center using the proposed blocks, the scour rate significantly increases at wall sides, causing heightened hole length.

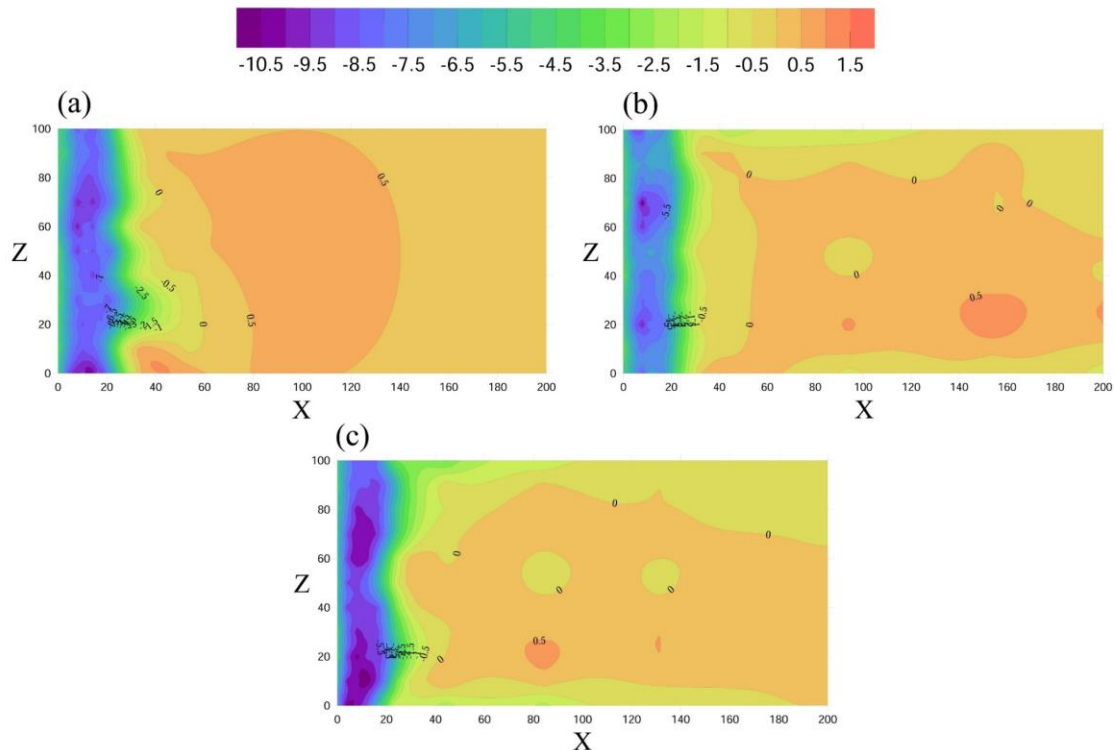


Figure 11. The bed topography of the chute without divergence at a discharge rate of 15 L/s for (a) standard, (b) semicircular, and (c) trihedral blocks.

It is clear that the divergence ratio of the chute affects the rate and distribution of scour downstream of this structure. An asymmetric bed topography is observed due to transverse fluctuations of the flow in the constant-width chute. However, a relatively symmetric scour pattern is seen for the models with a divergence ratio of larger than 1. With elevation of the divergence ratio, the maximum scour hole is approached from the middle of the channel towards the side walls. Further, sedimentation pattern downstream of the scour hole is influenced by the chute divergence ratio and the Froude number upstream of the flow, were the most uniform scour and sedimentation pattern with the minimum depth of the scour hole is observed for DW2. Hence, one can conclude that with increasing the divergence ratio from 1 to 1.75 at a constant discharge rate of 9.5 L/s, the uniformity of the scour distribution and sedimentation downstream of the structure grows to a large extent. However, with further increase of the divergence ratio to 2.45, as the Froude number and consequently the surface flow velocity increases and causes over-turbulence, a non-uniform scour pattern is again formed, leading to an increase in the maximum scour hole and point bar height. The effect of various parameters affecting the scour hole is discussed in the following sections.

3.2. The mean and maximum depth of the scour hole

Figure 12 reveals the changes in the mean and maximum depth of the scour hole at different divergence ratios for different block geometries at different Froude numbers upstream of the chute

under various conditions. Figure 12(a) indicates the relationship between the changes in the dimensionless mean depth of the scour hole at different Froude numbers for the flow over the chute. Clearly, the maximum mean depth of the scour hole is observed for the standard blocks without inlet divergence. With elevation of (b_2/b_1) from 1 to 2.45 and changing the block geometry from standard to semicircular and trihedral blocks, the mean and maximum depths of the scour hole significantly diminished by up to 50 and 40%, respectively, as a result of the increased Froude number.

At a constant Froude number upstream of the chute, the maximum and minimum mean scour depths were observed for the model without divergence and with standard blocks respectively and that with a divergence ratio of 2.45 with semicircular blocks. The effect of block geometry on the structure performance was also investigated. According to the results, at all divergence ratios and the cases with no divergence, except for $(b_2/b_1=1.75)$, the semicircular block outperformed other geometries in terms of reducing the mean depth of the scour hole depth, in particular at Froude numbers less than 0.25.

Figure 12(b) indicates the maximum depth of the scour hole for various models at different upstream Froude numbers. In general, with increase in the Froude number, the maximum depth of the scour hole for all blocks grows at all divergence ratios, but at different rates for different models. At a constant Froude number, the maximum scour hole depth was observed for the non-divergent model $(b_2/b_1=1)$ with standard blocks, while the minimum scour depth was found for the model with a divergence ratio (b_2/b_1) of 2.45 with semicircular blocks. It can be concluded that despite the divergence at chute inlet, semicircular blocks may cause a significant reduction in the maximum and mean depths of the scour hole in comparison with trihedral and standard USBR blocks. This can be related to the semicircular geometry of the blocks reducing the dimensions of the scour hole through extreme turbulence and increased energy dissipation.

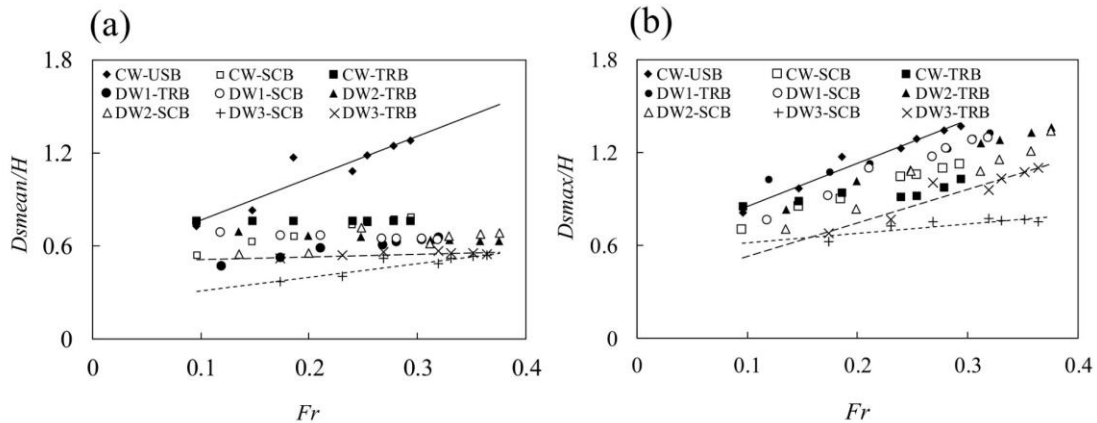


Figure 12. The changes in the dimensionless ratio with the Froude number: (a) mean depth of the scour hole, (b) maximum depth of the scour hole.

3.3. The mean and maximum length of the scour hole

Figures 13(a) and 13(b) represent the changes in the maximum and mean lengths of the scour hole respectively at various divergence ratios for different block types at different Froude numbers upstream of the chute under different conditions. As clearly seen, with elevation of the

Froude number upstream of the chute, the maximum and mean lengths of the scour hole rose in all models.

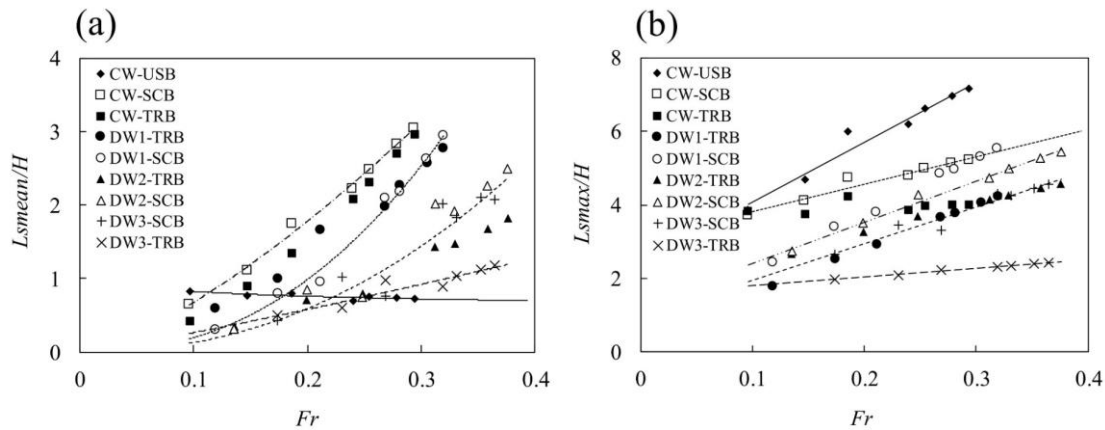


Figure 13. The changes in the dimensionless ratio with the Froude number: (a) the mean and (b) maximum length of the scour hole.

According to Figure 13(a), the mean length of the scour hole increases in all models except for the one with standard USBR blocks as the Froude number upstream of the chute grows. Given that the maximum scour hole length occurred in the CW-USB model, the reduction of the mean length of the scour hole can be attributed to the more significant reduction of the length of the scour hole than its length, causing a reduction in the mean length of the scour hole as the Froude number increased upstream of the chute.

Figure 13(b) compares the maximum length of scour holes formed by different block geometries. As can be seen, at each Froude number, the maximum length of the scour for standard blocks has been higher than that for semicircular and trihedral blocks. The difference in the maximum length of the scour hole grows with elevation of the Froude number upstream of the chute.

Further, with increase in the opening ratio (b_2/b_1) from 1 to 2.45, the maximum and mean lengths of the scour hole decreased from 45% to 60% and from 30 to 70% at Froude numbers of 0.1 and 0.3 respectively. Comparison of the performance of semicircular and trihedral blocks suggests that at each divergence ratio, the trihedral blocks have reduced the scour hole length by 40% more than the semicircular blocks did.

In general, one can conclude that semicircular blocks outperform standard and trihedral blocks in terms of reducing the maximum and mean depths of the scour hole. However, trihedral blocks outperformed other block geometries concerning reduction of the length of the scour hole.

3.4. Energy dissipation

Relative energy dissipation of the flow passing over the chute is shown in Figure 14 at different Froude numbers upstream of the chute. As seen, the relative energy dissipation falls with elevation of the Froude number, but with different downtrends in different models.

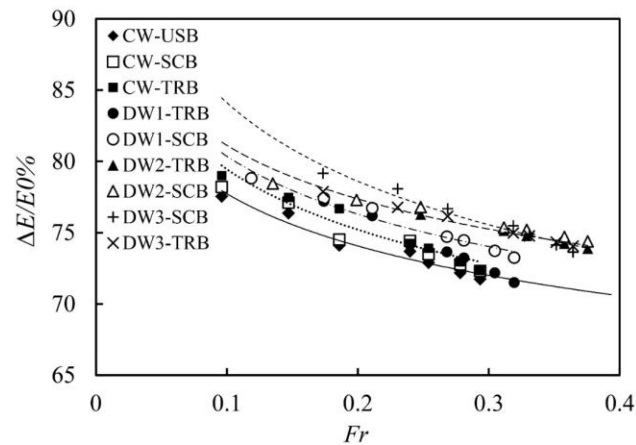


Figure 14. Relative energy dissipation at different Froude numbers upstream of the chute.

Generally speaking, the models with semicircular blocks show a higher relative energy dissipation at an identical opening ratio. The maximum energy dissipation was observed for the model with a semicircular block with a divergence ratio (b_2/b_1) of 2.45 (DW3-SCb). On the other hand, the model with standard blocks without divergence (CW-USB) showed the minimum energy dissipation. Thus, it can be concluded that with changing the block geometries from standard to semicircular blocks and the subsequent increase in the turbulence and energy dissipation, flow energy drops downstream of the chute, leading to a decrease in the dimensions of the scour hole. The models DW3-SCB and DW3-TRB show the maximum energy dissipation with the minimum length and depth of the scour hole. According to the results concerning the effect of divergence ratio on the relative energy dissipation, with increase in the divergence ratio from 1 to 2.45, the relative energy dissipation by the flow over the chute has grown by 4% to 8%, presumably due to flow acceleration upstream of the chute in response to inlet divergence and the subsequent increase in turbulence from collision of the flow with the middle blocks. This can ultimately lead to increased energy dissipation thereby forming smaller scour holes.

4. Conclusion

The effects of divergence ratio of a baffled chute and the geometry of blocks installed on the chute were investigated on the scour hole pattern and dimensions downstream of the chute. For this purpose, semicircular and trihedral blocks were proposed as alternatives to standard USBR blocks and the effect of blocks of different geometries on scour downstream of the chute was then investigated. The effect of three divergence ratios (b_2/b_1) of 1, 1.45, and 2.45 at chute inlet was also examined. According to the results, with increase in the inlet divergence ratio for all block geometries, the scour hole and point bars showed a greater asymmetry and more uniform topography relative to the flume centerline. Elevation of the divergence ratio from 1 to 2.45 caused a significant reduction in the mean and maximum depth of the scour hole. The use of standard USBR blocks at a constant chute width caused the maximum depth of the scour hole to occur in the middle of the channel. However, the proposed semicircular and trihedral blocks shifted the maximum scour depth towards the side walls. This can be related to the geometry of blocks forming secondary eddy currents due to the wall curvature. Collision of eddy currents with

the side walls and the subsequent formation of horseshoe-shaped vortices result in scouring of the side walls in addition to extending the hole on both sides of the channel in the vicinity of the side walls. This may endanger wall stability and should be further studied. Comparison of the results indicated that as the geometry changed from standard USBR to semicircular blocks, the mean depth of the scour hole decreased by 50%. According to the results on the effect of inlet divergence ratio, the divergence caused formation of more asymmetric scour holes with a lower length and depth. Finally, as the divergence ratio rose from 1 to 2.45, energy dissipation grew by 8% due to a reduction in the scour hole dimensions.

References

1. Bormann, N. E.; Julien, P. Y. Scour downstream of grade-control structures. *Journal of Hydraulic Engineering*. Vol.117, No. 5, 1991, 579-594.
2. Chanson, H.; Toombes, L. Energy dissipation and air entrainment in stepped storm waterway: experimental study. *Journal of Irrigation and Drainage Engineering*. Vol.128, No. 5, 2002, 305-315.
3. D'Agostino, V.; Ferro, V. Scour on alluvial bed downstream of grade-control structures. *Journal of Hydraulic Engineering*. Vol.130, No. 1, 2004, 24-37.
4. Dargahi, B. Scour development downstream of a spillway. *Journal of Hydraulic Research*, Vol.41, No. 4, 2003, 417-426.
5. Elnikhely, E. Investigation and analysis of scour downstream of a spillway. *Ain Shams Engineering Journal*, No, 2017.
6. Farhoudi, J., Smith, K. V. Local scour profiles downstream of hydraulic jump. *Journal of Hydraulic Research*, Vol. 23, No. 4, 1985, 343-358.
7. Kaya, N. Emiroglu, M. E. Study of oxygen transfer efficiency at baffled chutes. presented at the meeting of Proceedings of the Institution of Civil Engineers-Water Management, 2010, 447-456, Thomas Telford Ltd.
8. Novak, P. Influence of bed load passage on scour and turbulence Downstream of stilling basin. presented at the meeting of 9th Congress, IAHR, 1961, Dubrovnik, Croatia.
9. Pagliara, S.; Palermo, M. Influence of tailwater depth and pile position on scour downstream of block ramps, *Journal of Irrigation and Drainage Engineering*, Vol.136, No. 2, 2009, 120-130.
10. Pagliara, S.; Palermo, M. Effect of stilling basin geometry on clear water scour morphology downstream of a block ramp, *Journal of Irrigation and Drainage Engineering*, Vol.137, No. 9, 2010, 593-601.
11. Pagliara, S.; Palermo, M. Effect of stilling basin geometry on the dissipative process in the presence of block ramps, *Journal of Irrigation and Drainage Engineering*, Vol.138, No. 11, 2012, 1027-1031.
12. Peterka, A. Hydraulic Design of Stilling Basins and Energy Dissipators, Engineering Monograph No. 25, U.S. Department of Interior, Bureau of Reclamation, 1964, 154-188.
13. Tuna, M. Effect of offtake channel base angle of stepped spillway on scour hole, *Iranian Journal of Science and Technology, Transactions of Civil Engineering*, Vol.36, No. C2, 2012, 239.
14. Zare, H. K., Doering, J. C. Energy dissipation and flow characteristics of baffles and sills on stepped spillways, *Journal of Hydraulic Research*, Vol.50, No. 2, 2012, 192-199.